

A quantum fluid of metallic hydrogen suggested by first-principles calculations

Stanimir A. Bonev*, Eric Schwegler,
Tadashi Ogitsu & Giulia Galli

Lawrence Livermore National Laboratory, University of California, Livermore, California 94550

It is generally assumed^{1,2,3} that solid hydrogen will transform into a metallic alkali-like crystal at sufficiently high pressure. However, some theoretical models^{4,5} have also suggested that compressed hydrogen may form an unusual two-component (protons and electrons) metallic fluid at low temperature, or possibly even a zero-temperature liquid ground state. The existence of these new states of matter is conditional on the presence of a maximum in the melting temperature versus pressure curve (the 'melt line'). Previous measurements^{6,7,8} of the hydrogen melt line up to pressures of 44 GPa have led to controversial conclusions regarding the existence of this maximum. Here we report *ab initio* calculations that establish the melt line up to 200 GPa. We predict that subtle changes in the intermolecular interactions lead to a decline of the melt line above 90 GPa. The implication is that as solid molecular hydrogen is compressed, it transforms into a low-temperature quantum fluid before becoming a monatomic crystal. The emerging low-temperature phase diagram of hydrogen and its isotopes bears analogies with the familiar phases of ³He and ⁴He, the only known zero-temperature liquids, but the long-range Coulombic interactions and the large component mass ratio present in hydrogen would ensure dramatically different properties^{9,10}.

The possible existence of low-temperature liquid phases of compressed hydrogen has been rationalized with arguments based on the nature of effective pair interactions and of the quantum dynamics at high density, resulting in proton-proton correlations insufficient for the stabilization of a crystalline phase⁵. But so far there has been no conclusive evidence establishing whether hydrogen metallizes at low temperature as a solid (the more widely accepted view to date) or as a liquid. Measurements and theoretical predictions of the near-ground state high-pressure phases³ of hydrogen have proven to be difficult because of the light atomic mass, significant quantum effects and strong electron-ion interactions. In this regard, the finite temperature liquid-solid phase boundary predicted here is especially valuable for understanding the manner in which hydrogen metallizes.

The appearance of a maximum melting temperature in hydrogen is in itself a manifestation of an unusual physical phenomenon. The few systems with a negative melt slope involve either open crystalline structures, such as water and graphite, or in the case of closed packed solids, a promotion of valence electrons to higher orbitals upon compression (6s to 5d in cesium¹¹, for example). In these cases, the liquid is denser than the solid when they coex-

ist, possibly because of structural or electronic transitions taking place continuously in the liquid, as a function of pressure, but only at discrete pressure intervals in the solid.

In contrast, recent experiments⁸ have shown that hydrogen phase I – a solid structure with rotationally-free molecules associated with the sites of a hexagonal closed packed (hcp) lattice – persists below the liquid transition up to at least 150 GPa, i.e. well beyond the melt curve maximum predicted here. The promotion of electrons to higher orbitals in hydrogen can also be ruled out because of the prohibitive high energy involved. Alternatively, it has been suggested that dissociation in the fluid, either gradual⁷ or following a first-order liquid-liquid (LL) phase transition^{12,13}, may be the origin of a maximum in the melt line. This idea is not supported by our results. Instead, we explain the physical origin of the maximum in terms of changes in the *intermolecular* interactions – a mechanism significantly different from that expected from familiar phenomenological models.

The approach taken here to compute the melt line is one of direct simulation of the melting process. Hysteresis effects of super-heating or super-cooling during the phase transition are avoided by simulating solid and liquid phases in coexistence. The validity of this method

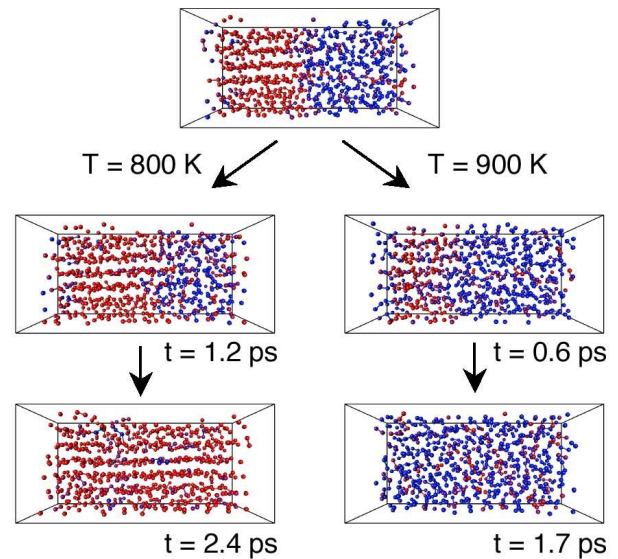


FIG. 1: Snapshots from two-phase MD simulations at $P = 130$ GPa and temperatures below and above the melting temperature. A quantitative assessment of the instantaneous local order environment around each molecule has been performed as described in Ref. 17, and compared with single-phase solid and liquid simulations. Molecules are coloured according to the arrangement of their nearest neighbours, red and blue representing configurations uniquely characteristic of the hcp solid and liquid at the given P and T , respectively (the Q_4 order parameter¹⁷ has been used for the colour map). The systems reach equilibrium at the target average temperatures (800 and 900 K) over a time interval of ~ 0.5 ps, which is followed by periods of coexistence lasting from 1 to several picoseconds. The phase transitions are observed by monitoring changes in the diffusion constants, pair correlation functions, specific volumes and local order parameters. In addition, some noticeable correlations between temperature and diffusion variations indicate the exchange of latent heat.

is then assessed by reducing size effects in such a way that realistic thermodynamic processes can be mimicked. This technique, known as two-phase simulation, has been mostly applied with model potentials¹⁴, thus allowing the simulation of large systems, and only recently it was demonstrated^{15,16} that implementations within the framework of first principles molecular dynamics (MD) are feasible.

Two-phase simulations (Fig. 1) are performed for various pressure and temperature conditions to predict the melt curve of hydrogen up to 200 GPa (Fig. 2). As discussed in Refs. 7 and 8, the experimental data available up to 44 GPa can be equally well fitted with several empirical melt equations, leading to qualitatively different conclusions regarding the further rise or fall of the phase boundary. Our results at 50 GPa compare favourably with recent measurement⁸, and the calculations at 130 and 200 GPa predict a negative slope in this pressure region.

Previous first-principles calculations^{12,19} indicated the existence of a sharp transition from molecular to non-molecular fluid, thus raising the possibility that the melt curve maximum is a liquid-liquid-solid triple point. We therefore studied the properties of the liquid at temperatures above melting. In our simulations, we do find

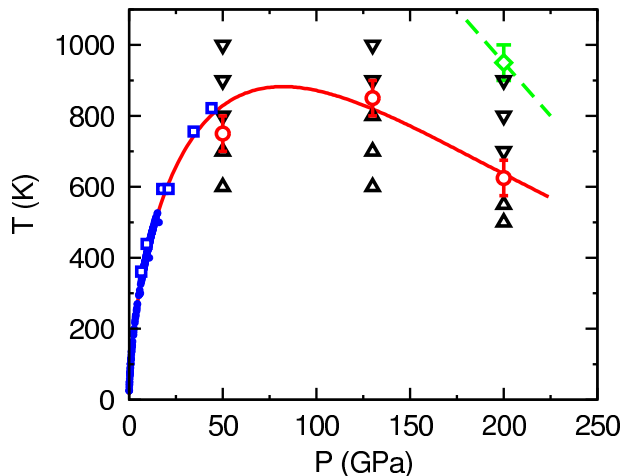


FIG. 2: Melt curve of hydrogen predicted from first principles MD. The filled circles are experimental data from Refs. 6 and 7 and references therein, and the open squares are measurements from Ref. 8. Triangles indicate two-phase simulations where solidification (up) or melting (down) have been observed, and bracketed melting temperatures (T_m) are represented by open circles. As the phase boundary is approached, the period of coexistence increases and eventually the outcome becomes dependent on the choice of simulation parameters. This degree of arbitrariness is reflected in the error bars of T_m , which also include the standard deviation of the temperatures collected during the MD simulations. All experimental and theoretical points are given equal weight and fitted with a Kechin melt equation¹⁸ (solid line in the figure): $T_m = 14.025 (1 + P/a)^b \exp(-cP)$ K, where P is in units of GPa, $a = 0.030355$, $b = 0.59991$, and $c = 0.0072997$. The open diamond marks the liquid-liquid transition from molecular to non-molecular fluid at 200 GPa, and the estimated slope of this phase boundary is given by the dashed line. The error bar on the diamond symbol indicates the hysteresis effects during the simulation of the liquid-liquid transition.

a first-order liquid-liquid phase transition from molecular to dissociating fluid, but this occurs at temperatures higher than those of the melting line; at 200 GPa, the liquid-liquid transition takes place between 900 and 1,000 K (Fig. 2). Thus, in the entire pressure range considered here, the liquid remains molecular below 900 K, with molecules stable over the simulation times of several picoseconds. We emphasize that on heating above a critical temperature, the transition to a non-molecular fluid takes place very rapidly, over a couple of hundred femtoseconds of simulation time. When the fluid is subsequently quenched, the molecules recombine and the system reverts to the molecular state. Therefore, we conclude that the change from a positive to a negative melt line slope happens gradually and we emphasize that it is not directly related to molecular dissociation. However, extrapolations of the melt line and the liquid-liquid phase transition indicate a triple point at ~ 300 GPa and 400 K. Above this pressure, the solid is expected to melt into a metallic liquid.

To estimate the errors originating from finite system size effects, we have computed the ground state pressure and energy for different size simulation cells sampled at the the Γ -point and with a $2 \times 2 \times 2$ k-point mesh. The pressure and energy *differences* between the solid and the liquid are converged to within 0.3 GPa and 1 meV

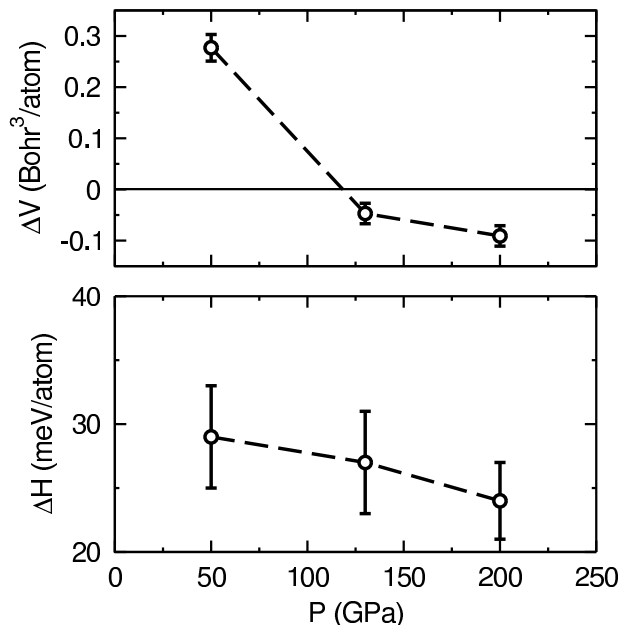


FIG. 3: Difference of the specific volumes (ΔV) and enthalpies (ΔH) between the liquid and solid phases at the melting temperatures determined from the two-phase simulations. The reported uncertainties include standard deviations collected during the MD simulations and observed size effects from single-phase simulations with 360 and 768 atom supercells. The data are used to compute melt slopes from the Clausius-Clapeyron equation: $dT_m/dP = T_m \Delta V / \Delta H$; the values obtained for 50, 130 and 200 GPa are (6.5 ± 1.2) , (-1.4 ± 0.6) and (-2.3 ± 0.6) K/GPa, respectively. For comparison, the slopes from the melt line fit in Figure 2 are 3.9, -2.2 and -2.7 K/GPa, but we note that these are weighted heavily by the experimental data, especially at lower pressure.

per ion, and the estimated errors are included in Fig. 3. A question that remains to be answered is whether the size of the system considered here is sufficient to simulate liquid-solid coexistence. To address this, we carried out MD simulations of single-phase solid and liquid hydrogen at the melting temperatures determined in the two-phase simulations. The differences in the specific volumes and enthalpies obtained in this way (Fig. 3) are then used to compute the melt slopes using the Clausius-Clapeyron equation. The agreement with the results from two-phase simulations gives us confidence that the computed melt curve is thermodynamically consistent.

We also discuss the validity of the principal approximations in our theoretical method: (1) adiabatic interactions, (2) the generalized gradient approximation (GGA) for the exchange-correlation energy, and (3) classical treatment of ion motion. Electron-phonon interactions are significant in the solid phase when the direct band gap is comparable with the phonon frequencies; an event that eventually occurs at high densities. But at 200 GPa and 600 K – the conditions examined here where the electron-phonon coupling is expected to be most pronounced – the GGA band gap is still ~ 2 eV. We note that the GGA tends to systematically underestimate band gaps; this has been shown for various materials, including hydrogen²⁰. However, because the highest vibrational frequencies in hydrogen are ~ 0.5 eV, the computed GGA band gap – a lower bound to the actual value – is already sufficient to establish that non-adiabatic effects are indeed negligible.

Local density approximations are also expected to favour the phase with more delocalised electrons; previous studies have shown a consistent tendency of the GGA to underestimate melting temperatures, such as those of lithium hydride¹⁵ and aluminium¹⁶. Here, this effect is expected to be very small because the molecular bonding properties and the atomic coordination differ little in the solid and liquid phases. This also implies that the zero-point energy bound in the vibron motion is similar in the two phases. Indeed, velocity-velocity autocorrelation analysis carried out on our MD trajectories shows that vibron frequency distributions (containing all vibrational modes) differ by less than 10 cm^{-1} in the solid and the liquid between 50 and 200 GPa. In addition, we have computed the first-order quantum correction to the ionic free energies. It is given by the Wigner-Kirkwood formula, $\Delta F = \hbar^2 / (24k_B^2 T^2) \sum_i \langle \mathbf{F}_i^2 \rangle / m_i$, where the average is over the classical ensemble, and \mathbf{F}_i and m_i are the ionic forces and masses. The *difference* in the quantum corrections for the two phases obtained in this way at pressures of 50, 130 and 200 GPa remains less than 2 meV for temperatures near the computed melt curve.

We now turn our attention to the physical origin of the maximum in the melt curve of hydrogen. The transition from an ordered to a disordered state is governed by the relative importance of entropy and energy. At high pressure, the interactions become mostly repulsive, and it is reasonable to expect that a deviation from a crystalline arrangement becomes progressively more unfavourable in terms of enthalpy. This is indeed the case for most materials, as is reflected in the positive slopes of their melt curves. On the other hand, attractive many-

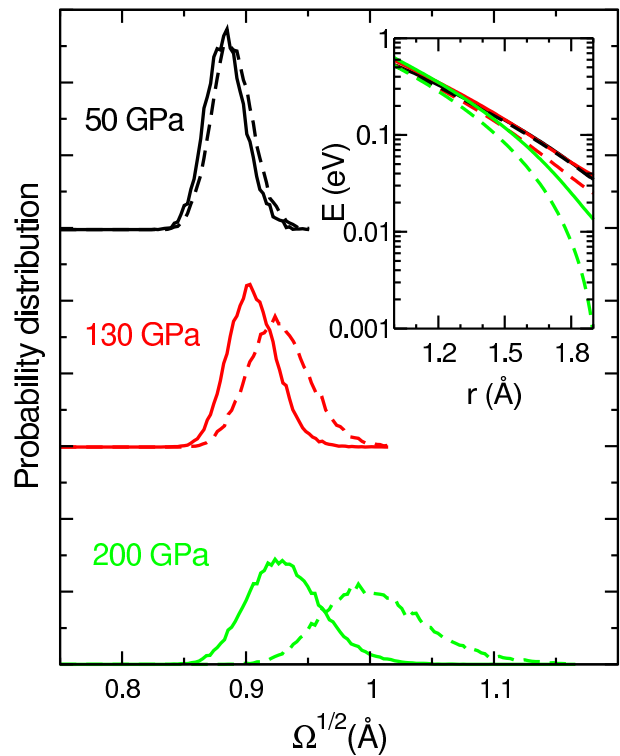


FIG. 4: The probability distribution of MLWF spreads²⁴ at $T=700$ K and $P=50$ (black curves), 130 (red curves) and 200 GPa (green curves). The solid and dashed curves correspond to distributions collected from the solid and liquid phases, respectively. The inset shows the effective hydrogen-hydrogen potentials obtained directly from the simulation trajectories with the force-matching procedure described in Ref. 26 (the same coloring has been used). As the pressure is increased, the spreads of the MLWF are shown to increase faster in the liquid than in the solid phase. In addition, effective potentials soften more quickly in the liquid than in the solid phase at the nearest neighbor molecular separation distance. Note that the potentials at 50 GPa in the liquid and solid phases, and at 130 GPa in the solid phase, are indistinguishable on this scale.

body interactions can soften the steep increase of the repulsive forces at high density^{21,22}. Although, in principle, such a softening opens up the possibility for a melt curve maximum²³, it does not appear to be a sufficient condition for its existence. Indeed, softening of the repulsive part of the pair potentials has been observed for a number of materials for which there is no experimental indication of a melt line turnover. As will be shown below, the physics behind the unique melt curve of hydrogen is related to the *different rate* at which the repulsive interactions (at intermolecular range) are weakened in the solid and liquid phases as a function of pressure.

To investigate how many-body interactions give rise to repulsive force softening in the liquid and the solid, we have performed an analysis based on maximally-localized Wannier functions (MLWF). These functions have been shown²⁴ to provide an intuitive description of chemical bonds in condensed phases and they have recently been used²⁵ to investigate the infrared activity of candidate structures of hydrogen phase III. We have computed MLWF along the 700 K isotherm, at various pressures, and find that their spreads (Fig. 4) increase faster in the

fluid than in the solid, as the system is compressed. Importantly, the differences in the two phases come from the tails of the MLWF, while their profiles around the centres of the molecular bonds remain nearly the same. Therefore, the large MLWF spread observed in the high-pressure fluid comes from the increased overlap of the molecular orbitals, here represented by the MLWF. Because the specific volumes of the solid and the liquid are very similar under the conditions examined here, the physical origin of the larger spread in the fluid can be attributed to the disorder in the liquid phase. Furthermore, the tails of the MLWF in the fluid are characterized by an asymmetry, which can be viewed as an effective intermolecular charge transfer, giving rise to an enhanced infrared activity in the liquid phase.

The properties of the MLWF found in our calculations are indicative of the behaviour of repulsive interactions in the solid and liquid as a function of pressure. Effective hydrogen-hydrogen pair potentials derived from our *ab initio* MD trajectories using a force matching technique²⁶ are displayed in the inset of Fig. 4. As in the MLWF behaviour, we observe a stronger softening of the potential in the liquid than in the solid. Our Wannier function analysis indicates that this increased softening is the result of charge transfer processes, enhanced by disorder, which appear to have a qualitative character similar to those proposed in Ref. 27 for phase III of solid hydrogen. We also note that the attenuation of repulsive interactions observed here in the solid phase correlates well with the analysis of Raman spectroscopic data²⁸, which has indicated softening of the effective intermolecular force constants above ~ 100 GPa.

To summarize, we have predicted the melt curve of hydrogen between 50 and 200 GPa from first principles. Above approximately 82 GPa, the melt line has a negative slope – a phenomenon that we have related to softening of the intermolecular interactions, which occur at a faster rate in the liquid than in the solid, as a function of pressure. Our results provide strong evidence that above ~ 300 GPa the solid melts into a metallic liquid and that a low-temperature metallic quantum fluid will exist at pressures near 400 GPa. Although we have only directly probed temperatures as low as 600 K, our conclusions are likely to hold at lower temperatures as well. Indeed, quantum ion motion usually favours phases with lower ion-ion correlations, which would further stabilize the low-temperature liquid phase found here. In addition, our findings are consistent with pressure estimates from experiments where hydrogen is expected to metallize^{3,29}. Finally, we note that the observed increase in MLWF spreads when going from the high-pressure solid to the molecular liquid phase points at the presence of dynamically-induced intermolecular charge transfer (dipole moments); this indicates that the transition

from solid to liquid at high pressure is accompanied by an increase of the hydrogen infrared absorption. Therefore, we propose that measurements of infrared activity could be used to verify experimentally the predicted turnover of the melt curve.

Methods

Molecular dynamics

Our *ab initio* MD simulations are carried out with the GP code, written by F. Gygi, and using the Car-Parrinello (CP) method³⁰; the many-body electron problem was solved quantum-mechanically within the generalized gradient approximation³¹ of density functional theory, while the ions are propagated classically (the validity of this approximation for the problem at hand is discussed in the text). The actual calculations are performed for deuterium instead of hydrogen. The reason for this is that in the classical-ion picture, for the quantities of relevance here there is no distinction between hydrogen and its isotopes, but the substitution with heavier ions allows us to integrate the equations of motion with reasonably large time steps: 2 and 3 a.u. (1 a.u. = 0.0242 fs) depending on the density. Furthermore, we use a Γ -point sampling of the Brillouin zone, Troullier-Martins pseudopotentials, and 60 Ry energy cut-off for the plane wave expansion of the Kohn-Sham orbitals. The accuracy and transferability of our pseudopotential has previously been extensively tested¹⁹. We have explicitly verified that the electrons remain near the Born-Oppenheimer surface throughout the simulations by comparing pressures determined in the CP runs with those determined by fully optimizing wavefunctions for the same ionic trajectories. The use of CP-MD results in a systematic shift of about 0.5 GPa both in the solid and liquid phases.

Two-phase simulations

We perform the two-phase simulations by equilibrating solid (in the hcp structure) and liquid phases separately in 360-atom supercells with fixed geometry and applied periodic boundary conditions. The atomic arrangements obtained in this way are then merged, and the liquid and solid parts of the resulting 720-atom supercells are also heated independently to reduce the strain near the newly-formed interface. The whole equilibration process typically lasts for several picoseconds of simulation time. The MD runs of coexisting phases are then performed in the $N - P - T$ ensemble (constant number of particles, pressure and temperature respectively). The actual system being simulated initially represents semi-infinite alternating slabs (by applying periodic boundary conditions) of solid and liquid, but by the end of the runs only one of the two phases, the one that is stable at the chosen P and T , fills the entire volume.

* Present address: Department of Physics, Dalhousie University, Halifax, Nova Scotia B3H 3J5, Canada.

¹ Wigner, E. & Huntington, H. B. On the possibility of metallic modifications of hydrogen. *J. Chem. Phys.* **3**, 764-770 (1935).

² Ashcroft, N. W. Metallic hydrogen: A high-temperature superconductor? *Phys. Rev. Lett.* **21**, 1748-1799 (1968).

³ Mao, H. K. & Hemley, R. J. Ultrahigh-pressure transitions in solid hydrogen. *Rev. Mod. Phys.* **66**, 671-692 (1994).

⁴ Brovman, E. G., Kagan, Yu. & Kholas, A. Properties of

- metallic hydrogen under pressure. *Sov. Phys. JETP* **35**, 783-792 (1972).
- ⁵ Ashcroft, N. W. The hydrogen liquids. *J. Phys.: Condens. Matter* **12**, A129-137 (2000).
 - ⁶ Diatschenko, V. *et al.* Melting curves of molecular hydrogen and molecular deuterium under high pressures between 20 and 373 K. *Phys. Rev B* **32**, 381-389 (1985).
 - ⁷ Datchi, F., Loubeyre, P. & LeToullec, R. Extended and accurate determination of the melting curves of argon, helium, ice (H₂O) and hydrogen (H₂). *Phys. Rev B* **61**, 6535-6546 (2000).
 - ⁸ Gregoryanz, E., Goncharov, A. F., Matsuishi, K., Mao, H.-k., & Hemley, R. J. Raman spectroscopy of hot dense hydrogen. *Phys. Rev. Lett.* **90**, 175701 (2003).
 - ⁹ Ashcroft, N. W. Hydrogen at high density. *J. Phys. A: Math. Gen.* **36**, 6137-6147 (2003).
 - ¹⁰ Babaev, E., Sudbø, A., & Ashcroft N. W. A superconductor to superfluid phase transition in liquid metallic hydrogen. *Nature* **431**, 666-669 (2004).
 - ¹¹ Jayaraman, J., Newton, R. C. & McDonough, J. M. Phase relations, resistivity, and electronic structure of cesium at high pressure. *Phys. Rev.* **159**, 527-533 (1967).
 - ¹² Scandolo, S. Liquid-liquid phase transition in compressed hydrogen from first-principles simulations. *PNAS* **100**, 3051-3053 (2003).
 - ¹³ Kechin, V. V. Melting of metallic hydrogen at high pressure. *JETP Lett.* **79**, 46-49 (2004).
 - ¹⁴ Morris, J. R., Wang, C. Z., Ho, K. M. & Chan, C. T. Melting line of aluminum from simulations of coexisting phases. *Phys. Rev. B* **49**, 3109-3115 (1994).
 - ¹⁵ Ogitsu, T., Schwegler, E., Gygi, F. & Galli, G. Melting of lithium hydride under pressure. *Phys. Rev. Lett.* **91**, 175502 (2003).
 - ¹⁶ Alfe, D. First-principles simulations of direct coexistence of solid and liquid aluminum. *Phys. Rev. B* **68**, 064423 (2003).
 - ¹⁷ Steinhardt, P. J., Nelson, D. R. & Ronchetti M. Bond-orientational order in liquids and glasses. *Phys. Rev. B* **28**, 784-805 (1983).
 - ¹⁸ Kechin, V. V. Melting curve equations at high temperature. *Phys Rev. B* **65**, 052102 (2001).
 - ¹⁹ Bonev, S. A., Militzer, B. & Galli, G. Ab initio simulations of dense liquid deuterium: Comparison with gas-gun shock-wave experiments. *Phys. Rev. B* **69**, 104101 (2004).
 - ²⁰ Chacham, H., Zhu, X. & Louie, S. G. Pressure-induced insulator-metal transitions in solid xenon and hydrogen: A first-principles quasiparticle study. *Phys. Rev. B* **46**, 6688-6699 (1992).
 - ²¹ Hemley, R. J. *et al.* Equation of state of solid hydrogen and deuterium from single-crystal x-ray diffraction to 26.5 GPa. *Phys. Rev. B* **42**, 6458-6470 (1990).
 - ²² Nagao, K., Bonev, S. A., Bergara, A. & Ashcroft, N. W. Enhanced Friedel structure and proton pairing in dense solid hydrogen. *Phys. Rev. Lett.* **90**, 035501 (2003).
 - ²³ Yoshida, T. & Kamakura S. Liquid-solid transitions in systems of soft repulsive forces. *Progr. Theor. Phys.* **52**, 822-838 (1972).
 - ²⁴ Marzari, N & Vanderbilt, D. Maximally localized generalized Wannier functions for composite energy bands. *Phys. Rev. B* **56**, 12847-12856 (1997).
 - ²⁵ Souza, I., Martin, R. M., Marzari, N., Zhao, X. & Vanderbilt, D. Wannier-functional description of the electronic polarization and infrared absorption of high-pressure hydrogen. *Phys. Rev. B* **62**, 15505-15519 (2000).
 - ²⁶ Izvekov, S., Parrinello, M., Burnham, C. J., & Voth, G. A. Effective force fields for condensed phase systems from ab initio molecular dynamics simulations: A new method for force-matching. *J. Chem. Phys.* **120**, 10896-10913 (2004).
 - ²⁷ Hemley, R. J., Soos, Z. G., Hanfland & M., Mao, H. K. Charge-transfer states in dense hydrogen. *Nature* **369**, 384-387 (1994).
 - ²⁸ Moshary F., Chen N. H. & Silvera I. F. Pressure dependence of the vibron in H₂, HD, and D₂: Implications for inter- and intramolecular forces. *Phys. Rev. B* **48**, 12613-12619 (1993).
 - ²⁹ Loubeyre, P., Occelli, F. & LeToullec, R. Optical studies of solid hydrogen to 320 GPa and evidence for black hydrogen. *Nature* **416**, 613-617 (2002).
 - ³⁰ Car, R. & Parrinello, M. Unified approach for molecular dynamics and density-functional theory. *Phys. Rev. Lett.* **55**, 2471-2474 (1985).
 - ³¹ Perdew, J. P., Burke, K. & Ernzerhof M. Generalized gradient approximation made simple. *Phys. Rev. Lett.* **77**, 3865-3868 (1996).

Acknowledgments We gratefully acknowledge S. Izvekov for providing the force-matching routines that were used in analysis shown in the inset of Figure 4, and F. Gygi for many useful discussions. This work was performed under the auspices of the U.S. Dept. of Energy at the University of California/Lawrence Livermore National Laboratory.

Competing interests statement The authors declare that they have no competing financial interests.

Correspondence and requests for materials should be addressed to S.A.B. (bonev1@llnl.gov).